Third generation sfermion decays into Z and W gauge bosons: Full one-loop analysis

Abdesslam Arhrib[1,2] and Rachid Benbrik[2]

[1]*Département de Mathématiques, Faculté des Sciences et Techniques, B.P. 416 Tanger, Morocco*
[2]*LPHEA, Département de Physique, Faculté des Sciences-Semlalia, B.P. 2390 Marrakech, Morocco*

(Received 6 January 2005; published 4 May 2005)

The complete one-loop radiative corrections to third-generation scalar fermions into gauge bosons Z and $W^{\pm}$ is considered. We focus on $\tilde{f}_2 \to Z\tilde{f}_1$ and $\tilde{f}_i \to W^{\pm}\tilde{f}'_j$, $f, f' = t, b$. We include SUSY-QCD, QED, and full electroweak corrections. It is found that the electroweak corrections can be of the same order as the SUSY-QCD corrections. The two sets of corrections interfere destructively in some region of parameter space. The full one-loop correction can reach 10% in some supergravity scenario, while in model independent analysis like general the minimal supersymmetric standard model, the one-loop correction can reach 20% for large $\tan\beta$ and large trilinear soft breaking terms A_b.

DOI: 10.1103/PhysRevD.71.095001 PACS numbers: 14.80.Ly, 12.15.Lk

I. INTRODUCTION

Supersymmetric theories predict the existence of scalar partners to all known quarks and leptons [1]. In grand unified SUSY models, the third generation of scalar fermions, $\tilde{t}, \tilde{b}, \tilde{\tau}$, gets a special status; due to the influence of Yukawa-coupling evolution, the light scalar fermions of the third generation are expected to be lighter than the scalar fermions of the first and second generations. For the same reason, the splitting between the physical masses of the third generation may be large enough to allow the opening of the decay channels like $\tilde{f}_2 \to \tilde{f}_1 V$ and/or $\tilde{f}_2 \to \tilde{f}_1 \Phi$, where V is a gauge boson and Φ is a scalar boson.

Until now there is no direct evidence for SUSY particles, and under some assumptions on their decay rates, one can only set lower limits on their masses [2]. It is expected that the next generation of e^+e^- machines and/or hadron colliders (CERN LHC and Tevatron) could establish the first evidence for the existence of SUSY particles. Typically, scalar quarks can be produced copiously both at hadron and lepton colliders. They can in principle be discovered at future hadron colliders (LHC) up to masses in the 1–2 TeV range while sleptons would become invisible to LHC if heavier than $\sim$250 GeV or so [3], due to their weak coupling and a prominent background.

If SUSY particles would be detected at hadron colliders, their properties can be studied with high accuracy at a high-energy linear e^+e^- collider [4]. It is thus mandatory to incorporate effects beyond leading order into the theoretical predictions, both for production and decay rate, in order to match the experimental accuracy.

In this spirit, the next-to-leading order corrections to squark-pair production at proton colliders have been studied theoretically in [5] and found to increase the cross section. For e^+e^- machines, scalar-fermion production has been addressed in several studies and shown to be promising for precision analysis of sfermion properties with mass and mixing-angle reconstructions [4,6]. SUSY-QCD corrections to squark-pair production at e^+e^- annihilation were shown, a decade ago, to be large [7,8]. Recently, the full one-loop radiative corrections to the production of scalar muons, scalar electrons (near threshold) [9], and third-generation scalar fermions $\tilde{t}, \tilde{b}, \tilde{\tau}$ [10,11] have been addressed. For squark-pair production at e^+e^-, the leading and subleading electroweak (EW) Sudakov logarithms were investigated [12] and found to be large at high energy.

Similar studies have been carried out for the decays of SUSY particles. In particular, the QCD corrections to scalar quark decay into quarks plus charginos or neutralinos have been studied in [13], while the full one-loop analysis has been addressed in [14] and found to have important impact on the partial decay widths of scalar fermions. In Ref. [15], the QCD corrections to the decays of heavy scalar quarks into light scalar quarks and Higgs bosons are found to be of the order 10%–20%.

Obviously, most of the studies concentrated on the production and decay of light states $\tilde{t}_1$, $\tilde{b}_1$, and $\tilde{\tau}_1$, while heavier states received less attention [10,14–16]. These heavy states can be produced both at LHC and/or at the future e^+e^- linear colliders. The decay of the heavier state third-generation scalar fermions is more complicated than the light one. One can basically have four sets of two-body decays:

(i) Strong decay for stop and sbottom $\tilde{t}_2 \to t\tilde{g}$, $\tilde{b}_2 \to b\tilde{g}$; if these decays are kinematically open they are the dominant ones.

(ii) Decay to chargino and neutralino: $\tilde{f}_2 \to f\tilde{\chi}_i^0$, $\tilde{f}_2 \to f'\tilde{\chi}_i^+$.
If the splitting between light and heavy third-generation scalar fermions is large enough we may have the following decays:

(iii) $\tilde{f}_2 \to \tilde{f}_1\Phi^0$, $\Phi^0 = h^0, H^0, A^0$, and $\tilde{f}_2 \to \tilde{f}'_1 H^{\pm}$.

(iv) $\tilde{f}_2 \to \tilde{f}_1 Z^0$ and $\tilde{f}_i \to \tilde{f}'_j W^{\pm}$.

It has been shown in [17] that the decay modes $\tilde{f}_2 \to \tilde{f}_1 Z^0$ and $\tilde{f}_i \to \tilde{f}'_j W$, if open and under some assumptions, may be the dominant ones. References [17] also evaluated the genuine SUSY-QCD corrections and found them to be of the order -5%–-10%.

Note also that in several benchmark scenarios for SUSY searches, the bosonic decay of $\tilde{t}_i$ and $\tilde{b}_i$ may be dominant [18]. For example, in the SPS5 scenario the dominant bosonic decay have the following branching ratios [19]: $\mathrm{Br}(\tilde{b}_1 \to W^- \tilde{t}_1) = 81\%$, $\mathrm{Br}(\tilde{b}_2 \to W^- \tilde{t}_1) = 64\%$, and $\mathrm{Br}(\tilde{t}_2 \to Z^0 \tilde{t}_1) = 61\%$. While in the SPS1 scenario, we have $\mathrm{Br}(\tilde{b}_2 \to W^- \tilde{t}_1) = 34\%$ and $\mathrm{Br}(\tilde{t}_2 \to Z^0 \tilde{t}_1) = 23\%$.

It is the purpose of this paper to provide the complete one-loop radiative corrections to $\tilde{f}_2 \to \tilde{f}_1 Z^0$ and $\tilde{f}_i \to \tilde{f'}_j W$ including real-photon emission, and discuss their effects in combination with the SUSY-QCD corrections.

The paper is organized as follows. In the next section, we will first set the notations and give the tree-level results. Section III outlines the calculations and the on-shell renormalization scheme we will use. In Sec. IV, we will discuss the effects of radiative corrections for various types of sfermion decays, and we end with a short conclusion in Sec. V.

II. NOTATIONS AND TREE-LEVEL FORMULAS

First we summarize the MSSM parameters needed in our analysis, with particular attention given to the sfermion sector. In the MSSM, the sfermion sector is specified by the mass matrix in the basis $(\tilde{f}_L, \tilde{f}_R)$. In terms of the scalar mass $\tilde{M}_L$, $\tilde{M}_R$, the Higgs-Higgsino mass parameter μ, and the soft SUSY-breaking trilinear coupling A_f, the sfermion mass matrix squared reads as

$$\mathcal{M}^2_{\tilde{f}} = \begin{pmatrix} m_f^2 + m_{LL}^2 & m_{LR} m_f \\ m_{LR} m_f & m_f^2 + m_{RR}^2 \end{pmatrix} \tag{1}$$

with

$$m_{LL}^2 = \tilde{M}_L^2 + m_Z^2 \cos 2\beta (I_3^f - Q_f s_W^2), \tag{2}$$

$$m_{RR}^2 = \tilde{M}_R^2 + m_Z^2 \cos 2\beta Q_f s_W^2, \tag{3}$$

$$m_{LR} = (A_f - \mu (\tan\beta)^{-2I_3^f}). \tag{4}$$

$I_3^f = \pm 1/2$ and Q_f are the weak isospin and the electric charge of the sfermion $\tilde{f}$ and $\tan\beta = v_2/v_1$ with v_1, v_2 being the vacuum expectation value of the Higgs fields.

The Hermitian matrix equation (1) is then diagonalized by a unitarity matrix $R_{\tilde{f}}$, which rotates the current eigenstates $\tilde{f}_L$ and $\tilde{f}_R$ into the mass eigenstates $\tilde{f}_1$ and $\tilde{f}_2$ as follows:

$$\begin{pmatrix} \tilde{f}_1 \\ \tilde{f}_2 \end{pmatrix} = R_{\tilde{f}} \begin{pmatrix} \tilde{f}_L \\ \tilde{f}_R \end{pmatrix} = \begin{pmatrix} \cos\theta_f & \sin\theta_f \\ -\sin\theta_f & \cos\theta_f \end{pmatrix} \begin{pmatrix} \tilde{f}_L \\ \tilde{f}_R \end{pmatrix} \tag{5}$$

where θ_f is the mixing angle such as

$$\tan 2\theta_f = \frac{2 m_{LR} m_f}{m_{LL}^2 - m_{RR}^2}. \tag{6}$$

The mixing angle θ_f is proportional to the mass of the fermion f. In the case of the supersymmetric partners of the light fermions, the mixing between the current eigenstates can therefore be neglected. However, mixing between top squarks can be sizable and allows one of the two mass eigenstates to be much lighter than the top quark. Bottom squark and tau slepton mixing can also be significant if $\tan\beta$ is large.

The physical masses, with the convention $m_{\tilde{f}_1} < m_{\tilde{f}_2}$, are given by

$$m^2_{\tilde{f}_{1,2}} = m_f^2 + \frac{1}{2}\Big(m_{LL}^2 + m_{RR}^2 \mp \sqrt{(m_{LL}^2 - m_{RR}^2)^2 + 4 m_{LR}^2 m_f^2} \Big). \tag{7}$$

The sfermions sector can be parametrized either by the original parameters in the Lagrangian or by the physical masses $m_{\tilde{f}_i} = m_i$ and mixing angle θ_f. Since we are computing radiative corrections in an on-shell scheme, we will take the following set of physical parameters:

$$m_{\tilde{t}_2}, m_{\tilde{b}_1} m_{\tilde{b}_2}, \theta_t, \theta_b$$

together with μ and $\tan\beta$. Once those parameters are fixed, the light stop mass can be derived using the mass sum rule [16] as follows:

$$m^2_{\tilde{t}_1} = \frac{1}{\cos^2\theta_t} (m_W^2 \cos 2\beta - m^2_{\tilde{t}_2} \sin^2\theta_t + m^2_{\tilde{b}_2} \sin^2\theta_b + m^2_{\tilde{b}_1} \cos^2\theta_b + m_t^2 - m_b^2). \tag{8}$$

Of course, Eq. (8) receives one-loop radiative corrections which are not included in this analysis. However, it has been shown in [20] that the one-loop corrections can shift the tree-level mass by less than $\lesssim 10$ GeV.

The soft supersymmetry-breaking parameters A_f are then connected to the previous ones through

$$A_f = \mu (\tan\beta)^{-2I_f} + \frac{m^2_{\tilde{f}_1} - m^2_{\tilde{f}_2}}{m_f} \sin\theta_f \cos\theta_f. \tag{9}$$

When varying the SUSY parameters, we have to be careful that charge and color minima do not appear. To avoid such minima at tree level, A_f has to satisfy the following tree-level conditions [21]:

$$\begin{aligned} A_t^2 &< 3\Big(m^2_{\tilde{t}_1} + m^2_{\tilde{t}_2} + \frac{1}{2}\cos 2\beta m_Z^2 - 2m_t^2 + M^2_{H_2} + \mu^2 \Big), \\ A_b^2 &< 3\Big(m^2_{\tilde{b}_1} + m^2_{\tilde{b}_2} + \frac{1}{2}\cos 2\beta m_Z^2 - 2m_b^2 + M^2_{H_1} + \mu^2 \Big), \\ A_\tau^2 &< 3\Big(m^2_{\tilde{\tau}_1} + m^2_{\tilde{\tau}_2} + \frac{1}{2}\cos 2\beta m_Z^2 - 2m_\tau^2 + M^2_{H_1} + \mu^2 \Big) \end{aligned} \tag{10}$$

with $M^2_{H_2} = (m_A^2 + m_Z^2)\cos^2\beta - 1/2 m_Z^2$ and $M^2_{H_1} = (m_A^2 + m_Z^2)\sin^2\beta - 1/2 m_Z^2$. For numerical check of charge color breaking as well as the $b \to s\gamma$ constraint, we have used Suspect and Sdecay codes [22,23].

The interaction of the neutral gauge bosons γ and Z with the sfermion mass eigenstates is described by the Lagrangian

$$\begin{aligned}\mathcal{L} = & -ieA^\mu \sum_{i=1,2} Q_f \tilde{f}_i^* \overleftrightarrow{\partial}_\mu \tilde{f}_i - ig_s G_a^\mu \sum_{i=1,2} T^a \tilde{f}_i^* \overleftrightarrow{\partial}_\mu \tilde{f}_i \\ & + iZ^\mu \sum_{i,j=1,2} g_{Z\tilde{f}_i\tilde{f}_j} \tilde{f}_i^* \overleftrightarrow{\partial}_\mu \tilde{f}_j \\ & + iW^\mu \sum_{i,j=1,2} g_{W\tilde{f}_i\tilde{f}'_j} \tilde{f}_i^* \overleftrightarrow{\partial}_\mu \tilde{f}'_j \end{aligned} \tag{11}$$

with

$$\begin{aligned} g_{Z\tilde{f}_i\tilde{f}_j} &= -\frac{e}{s_W c_W}\{(I_3^f - Q_f s_W^2) R_{j1}^{\tilde{f}} R_{i1}^{\tilde{f}} - Q_f s_W^2 R_{j2}^{\tilde{f}} R_{i2}^{\tilde{f}}\}, \\ g_{W\tilde{f}_i\tilde{f}'_j} &= -\frac{e}{\sqrt{2}s_W} R_{i1}^f R_{j1}^{f'}. \end{aligned} \tag{12}$$

The tree-level decay width can thus be written as

$$\Gamma^0(\tilde{q}_i^\alpha \to \tilde{q}_j^\beta V) = \frac{(g_{V\tilde{f}_i\tilde{f}_j})^2 \kappa^3(m_i^2, m_j^2, m_V^2)}{16\pi m_V^2 m_i^3}, \tag{13}$$

with $\kappa(x, y, z) = (x^2 + y^2 + z^2 - 2xy - 2xz - 2yz)^{1/2}$.

III. RADIATIVE CORRECTIONS

A. Scalar fermions decay into gauge bosons at one loop

The Feynman diagrams for the one-loop virtual contributions are generically displayed in Fig. 1 ($v_{1,\ldots,10}$). These diagrams are to be supplemented by the external self-energy contributions for gauge bosons and scalar fermions $\tilde{f}_{i,j}$ (Fig. 2), which are part of the counterterm for vertices v_{11} (Fig. 1), to be added according to renormalization. In the generic notation, V, S, F denote all insertions of vector, scalar, and fermionic states.

At one-loop level, transitions between gauge bosons and scalar bosons like $W^\pm$-$H^\pm$, $W^\pm$-$G^\pm$, Z^0-A^0, Z^0-G^0 are present. Owing to Lorentz invariance, those mixings are proportional to p_V^μ momentum; then, since the vector gauge bosons W and Z are on-shell transverse, those transitions vanish. In what follows we will ignore vector-scalar boson mixing.

The full set of Feynman diagrams are generated and evaluated using the packages FEYNARTS and FORMCALC [24]. We have also used LOOPTOOLS and FF [25] in the numerical analysis.

We have evaluated the one-loop amplitudes in the 't Hooft-Feynman gauge. The one-loop amplitudes are ultraviolet (UV) and infrared (IR) divergent. The UV singularities are treated by dimensional reduction [26] and are compensated in the on-shell renormalization scheme. We have checked explicitly that the results are identical in using dimensional reduction and dimensional regularization. The IR singularities are regularized with a small fictitious photon mass δ.

In the case of $\tilde{f}_2 \to Z\tilde{f}_1$ decay, diagrams like v_5 (Fig. 1) with $V = \gamma$ or $V =$ gluon and diagram v_{11} (Fig. 1) are IR divergent. In v_{11} the IR divergence comes from the wave function renormalization of the scalar fermions. For $\tilde{f}_2 \to W\tilde{f}'_1$ decay, diagrams like $v_{3,\ldots,6}$ (Fig. 1) and v_{11} (Fig. 1), $V = \gamma$ or $V =$ gluon are IR divergent. For an IR-finite decay width we have to add the contribution from real-photon and real-gluon emission, $\tilde{f}_i \to \tilde{f}_j^* V\gamma$ and $\tilde{f}_i \to \tilde{f}_j^* Vg$.

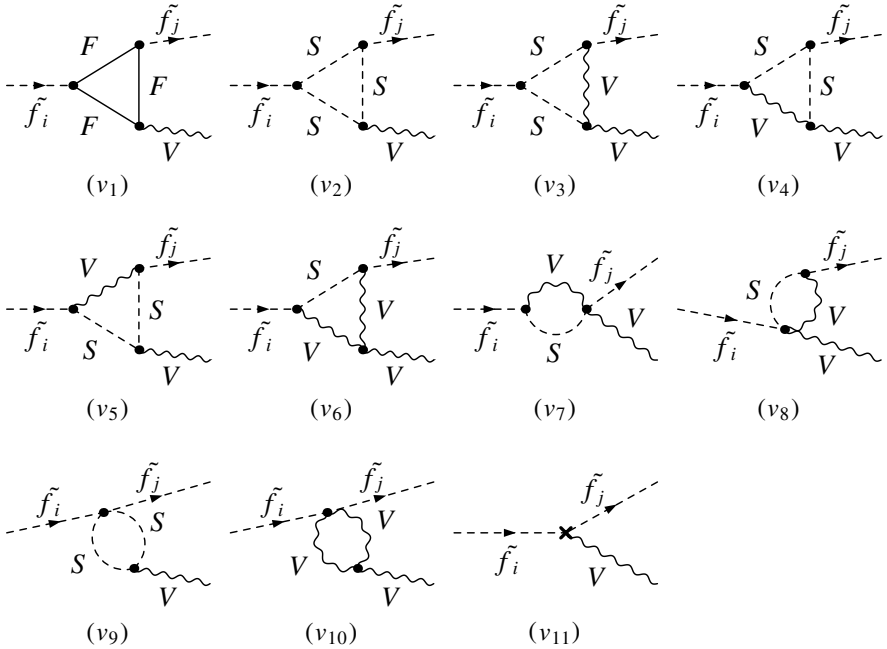

FIG. 1. Generic vertex contributions to $\tilde{f}_i \to \tilde{f}_j^* V$.

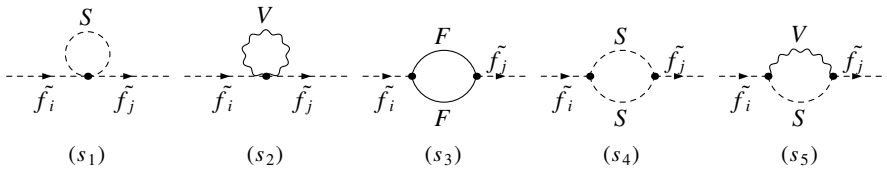

FIG. 2. Generic Feynman diagrams for scalar fermion self-energies $\tilde{f}_i \to \tilde{f}_j$.

B. Real-gluon emission

In order to cancel the infrared divergence coming from the virtual gluon, the real corrections with an additional gluon in the final state also need to be included. Feynman diagrams contributing to $\delta\Gamma_g^{br} = \Gamma(\tilde{q}_i \to \tilde{q}_j V g)$ are drawn in Fig. 3 (b_1, b_2, b_3). We would like to mention first, that in the present case and in all the following cases, we have checked that the gauge invariance is satisfied. The three body phase space integration is performed following Ref. [27], which yields a width[1]

$$\delta\Gamma_g^{br} = \frac{g^2_{V\tilde{f}_i\tilde{f}_j}\alpha_s}{4\pi^2 m_i}\frac{4}{3}\Big\{3I - \frac{\kappa^2}{m_V^2}[I_0 + I_1 + m_i^2 I_{00} + m_j^2 I_{11} + (m_i^2 + m_j^2 - m_V^2)I_{01}]\Big\}. \quad (14)$$

where $\kappa = \kappa(m_i^2, m_j^2, m_V^2)$, α_s is the strong coupling constant. The phase space integrals I, I_n, and I_{nm} have (m_i, m_j, m_V) as arguments. Their explicit forms are given in [27].

C. Real-photon emission

As in the case of the gluon, the infrared divergence coming from the virtual photon cancels out by including real (soft and hard) photon emission in the final state. The diagrams contributing to real bremsstrahlung of $\tilde{f}_i \to \tilde{f}_j Z$ are depicted in Fig. 3 (b_1, b_2, b_3).

In the case of $\tilde{f}_i \to \tilde{f}_j Z\gamma$, the width can be deduced from the gluon bremsstrahlung equation (14) just by replacing α_s in Eq. (14) by α, eliminating the QCD factor $\frac{4}{3}$ and multiplying by the square of scalar-fermion charges e_f^2. The width $\delta\Gamma_\gamma^{\rm br} = \Gamma(\tilde{q}_i \to \tilde{q}_j Z\gamma)$ is given by

$$\delta\Gamma_\gamma^{\rm br} = \frac{g^2_{Z\tilde{f}_i\tilde{f}_j}\alpha}{4\pi^2 m_i}e_f^2\Big\{3I - \frac{\kappa^2}{m_Z^2}[I_0 + I_1 + m_i^2 I_{00} + m_j^2 I_{11} + (m_i^2 + m_j^2 - m_Z^2)I_{01}]\Big\}, \quad (15)$$

where $e_d = -\frac{1}{3}$ for down squark and $e_u = \frac{2}{3}$ for up squark.

Finally, for the bremsstrahlung $\tilde{f}_i \to \tilde{f}'_j W\gamma$, the Feynman diagrams are drawn in Fig. 3 ($b_{1,\ldots,5}$). The decay width is more involved and is given by

$$\begin{aligned}\delta\Gamma_\gamma^{br} = {} & \frac{g^2_{W^\pm\tilde{f}_i\tilde{f}'_j}\alpha}{4\pi^2 m_i}\Big\{\frac{3}{4}(e_{f'} + e_f)^2 I - \frac{\kappa^2}{m_W^2}\Big[\frac{1}{2}e_f(e_{f'} + e_f)I_0 + \frac{1}{2}e_{f'}(e_{f'} + e_f)I_1 + e_f^2 m_i^2 I_{00} + e_{f'}^2 m_j^2 I_{11} \\ & + e_f e_{f'}(m_i^2 + m_j^2 - m_W^2)I_{01}\Big]\Big\} + \frac{\alpha}{8\pi^2 m_i}\{3(e_f + e_{f'})\{g^2_{W^\pm\tilde{f}_i\tilde{f}'_j}(-m_j^2 + m_i^2) + g_{G^\pm\tilde{f}_i\tilde{f}'_j}g_{W^\pm\tilde{f}_i\tilde{f}'_j}\}I_2 \\ & - \frac{1}{2}\{g^2_{W^\pm\tilde{f}_i\tilde{f}'_j}(\kappa^2 + 3m_W^2(1 - 2m_i^2 - 2m_j^2)) - 6g_{G^\pm\tilde{f}_i\tilde{f}'_j}g_{W^\pm\tilde{f}_i\tilde{f}'_j}(-m_j^2 + m_i^2) - 3g^2_{G^\pm\tilde{f}_i\tilde{f}'_j}\}I_{22} \\ & - \frac{\kappa^2}{m_W^2}e_f\{g^2_{W^\pm\tilde{f}_i\tilde{f}'_j}(m_i^2 - m_j^2 + 2m_W^2) + g_{G^\pm\tilde{f}_i\tilde{f}'_j}g_{W^\pm\tilde{f}_i\tilde{f}_j}\}I_{02} - \frac{\kappa^2}{m_W^2}e_{f'}\{g^2_{W^\pm\tilde{f}_i\tilde{f}'_j}(-m_i^2 + m_j^2 + 2m_W^2) \\ & + g_{G^\pm\tilde{f}_i\tilde{f}'_j}g_{W^\pm\tilde{f}_i\tilde{f}'_j}\}I_{12}\}\end{aligned} \quad (16)$$

with

$$\begin{aligned}g_{G^\pm\tilde{f}_i\tilde{f}'_j} = {} & \frac{g}{\sqrt{2}}\Big((m_W^2 c_{2\beta} + m_f^2 - m_{f'}^2)R^f_{i1}R^{f'}_{j1} \\ & + m_{f'}(\mu\tan\beta - A_{f'})R^f_{i1}R^{f'}_{1j} \\ & + m_f\Big(-\mu\frac{1}{\tan\beta} + A_f\Big)R^f_{i2}R^{f'}_{1j}\Big).\end{aligned} \quad (17)$$

[1]In the above Eq. (14), we found that the numerical factor in front of the I integral is 3 instead of 2 in Ref. [17]. This disagreement does not affect the numerical result at all.

D. On-shell renormalization

Recently, there have been several developments in the renormalization of MSSM. Several schemes are available [20,28–30]. Here, we follow the strategy of [14] by introducing counterterms for the physical parameters, i.e. for masses and mixing angles, and perform field renormalization in a way that residues of renormalized propagators can be kept at unity.

We will adopt throughout, the on-shell renormalization scheme of Refs. [27] for SM parameters and fields. We make the following prescriptions:

$$e \to (1 + \delta Z_e)e, \qquad M_{W,Z} \to M_{W,Z} + \delta M_{W,Z}; \quad (18)$$

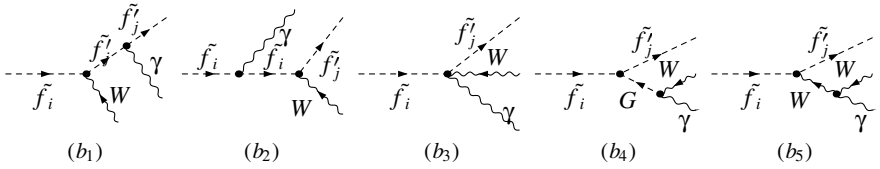

FIG. 3. Feynman diagrams for real-photon (or gluon) emission for the final state of $\tilde{f}_i \to \tilde{f}_j V\gamma$ (or $\tilde{f}_i \to \tilde{f}_j Vg$). In the case of $\tilde{f}_i \to \tilde{f}'_j W\gamma$ all diagrams $b_{1,\ldots,5}$ contribute, while for $\tilde{f}_i \to \tilde{f}_j Z\gamma$ only b_1, b_2, and b_3 contribute. In the case of QCD bremsstrahlung both for $\tilde{f}_i \to \tilde{f}'_j Wg$ and $\tilde{f}_i \to \tilde{f}_j Zg$ only b_1, b_2, and b_3 diagrams contribute.

the gauge bosons are renormalized such as

$$Z^\mu \to Z_{ZZ}^{1/2} Z^\mu + Z_{Z\gamma}^{1/2} A^\mu, \qquad A^\mu \to Z_{AA}^{1/2} A^\mu + Z_{\gamma Z}^{1/2} Z^\mu,$$
$$W^\mu \to \left(1 + \frac{1}{2}\delta Z_{WW}^{1/2}\right) W^\mu \tag{19}$$

with $Z_{ij}^{1/2} = \delta_{ij} + \frac{1}{2}\delta Z_{ij}$. In the on-shell scheme we use the mixing angle s_W (resp. c_W), which is defined by $s_W^2 = 1 - M_W^2/M_Z^2$ (resp. $c_W^2 = M_W^2/M_Z^2$). Its counterterm is completely fixed by the mass counterterms of W and Z gauge bosons as

$$\frac{\delta s_W}{s_W} = -\frac{1}{2}\frac{c_W^2}{s_W^2}\left(\frac{\delta M_W^2}{M_W^2} - \frac{\delta M_Z^2}{M_Z^2}\right),$$
$$\frac{\delta c_W}{c_W} = -\frac{1}{2}\left(\frac{\delta M_W^2}{M_W^2} - \frac{\delta M_Z^2}{M_Z^2}\right). \tag{20}$$

The extra parameters and fields we still have to renormalize in our case are the scalar-fermion wave functions $\tilde{f}_i$ and the mixing angle θ_f defined in Eq. (6).

In the general case, where sfermion mixing is allowed, the wave functions of the two sfermion mass eigenstates are not decoupled. Taking into account the mixing, the renormalization of the sfermion wave functions and the mixing angle θ_f can be performed by making the following substitutions in the Lagrangian equation (11):

$$\tilde{f}_1 \to Z_{11}^{1/2}\tilde{f}_1 + Z_{12}^{1/2}\tilde{f}_2, \qquad \tilde{f}_2 \to Z_{22}^{1/2}\tilde{f}_2 + Z_{21}^{1/2}\tilde{f}_1,$$
$$\theta_f \to \theta_f + \delta\theta_f. \tag{21}$$

Using the above prescriptions equations (18), (19), and (21) in the Lagrangian (11), the Lagrangian counterterm can be obtained and is given by

$$\delta\mathcal{L} = \sum_{i,j=1,2} [\delta(Z\tilde{f}_i\tilde{f}_j) Z^\mu \tilde{f}_i^* \overleftrightarrow{\partial}_\mu \tilde{f}_j + \delta(W\tilde{f}_i\tilde{f}'_j) W^\mu \tilde{f}_i^* \overleftrightarrow{\partial}_\mu \tilde{f}'_j] \tag{22}$$

where

$$\delta(Z\tilde{f}_i\tilde{f}_j) = -eQ_f\frac{1}{2}\delta Z_{\gamma Z} + g_{Z\tilde{f}_i\tilde{f}_j}\left(\delta Z_e + \frac{1}{2}\delta Z_{ZZ} + \frac{1}{2}\delta Z_{ii} + \frac{1}{2}\delta Z_{jj}\right) + \frac{\delta s_W e}{c_W^3 s_W^2}((-I_3^f - Q_f s_W^2 + 2I_3^f s_W^2) \times R_{j1}^{\tilde{f}} R_{i1}^{\tilde{f}} - Q_f s_W^2 R_{j2}^{\tilde{f}} R_{i2}^{\tilde{f}}) + g_{Z\tilde{f}_k\tilde{f}_j}\delta Z_{ki} + g_{Z\tilde{f}_i\tilde{f}_l}\delta Z_{lj} + \Delta(g_{Z\tilde{f}_i\tilde{f}_j})\delta\theta_f,$$
$$\delta(W\tilde{f}_i\tilde{f}'_j) = g_{W\tilde{f}_i\tilde{f}'_j}\left(\frac{\delta Z_{ii}}{2} + \frac{\delta Z_{jj}}{2}\right) + g_{W\tilde{f}_i\tilde{f}'_l}\frac{\delta Z_{lj}}{2} + g_{W\tilde{f}_k\tilde{f}'_j}\frac{\delta Z_{ki}}{2} + g_{W\tilde{f}_i\tilde{f}'_j}\left(\frac{\delta Z_{WW}}{2} + \frac{\delta s_W}{s_W} + \delta Z_e\right) - \Delta(g_{W\tilde{f}_i\tilde{f}'_j}) \tag{23}$$

where

$$\Delta(g_{Z\tilde{f}_1\tilde{f}_1}) = -\Delta(g_{Z\tilde{f}_2\tilde{f}_2}) = 2g_{Z\tilde{f}_1\tilde{f}_2},$$
$$\Delta(g_{Z\tilde{f}_1\tilde{f}_2}) = \Delta(g_{Z\tilde{f}_2\tilde{f}_1}) = g_{Z\tilde{f}_2\tilde{f}_2} - g_{Z\tilde{f}_1\tilde{f}_1},$$
$$\Delta(g_{W\tilde{f}_1\tilde{f}'_1}) = g_{W\tilde{f}_2\tilde{f}'_1}\delta\theta_f + g_{W\tilde{f}_1\tilde{f}'_2}\delta\theta_{f'},$$
$$\Delta(g_{W\tilde{f}_2\tilde{f}_2}\sim\sim) = -g_{W\tilde{f}_1\tilde{f}'_2}\delta\theta_f - g_{W\tilde{f}_2\tilde{f}'_1}\delta\theta_{f'},$$
$$\Delta(g_{W\tilde{f}_1\tilde{f}'_2}) = g_{W\tilde{f}_2\tilde{f}'_2}\delta\theta_f - g_{W\tilde{f}_1\tilde{f}'_2}\delta\theta_{f'},$$
$$\Delta(g_{W\tilde{f}_2\tilde{f}'_1}) = -g_{W\tilde{f}_1\tilde{f}'_1}\delta\theta_f + g_{W\tilde{f}_2\tilde{f}'_2}\delta\theta_{f'}. \tag{24}$$

To fix all the above renormalization constants, we use the following renormalization conditions:

(i) The on-shell conditions for m_W, m_Z, m_e and the electric charge e are defined as in the standard model [27].

(ii) The on-shell condition for the scalar fermion $\tilde{f}_i$: we choose to identify the physical scalar-fermion mass with the corresponding parameter in the renormalized Lagrangian, and require the residue of the propagators to have its tree-level value, i.e.,

$$\delta Z_{ii} = -\Re\left\{\frac{\partial}{\partial p^2}(\Sigma_{\tilde{f}_i\tilde{f}_i}(p^2))\right\}\Big|_{p^2=m_{\tilde{f}_i}^2},$$
$$\delta Z_{ij} = \frac{\Re\{\Sigma_{\tilde{f}_i\tilde{f}_j}(m_{\tilde{f}_j}^2)\}}{m_{\tilde{f}_j}^2 - m_{\tilde{f}_i}^2}, \qquad \delta m_{\tilde{f}_i}^2 = \Re(\Sigma_{\tilde{f}_i\tilde{f}_j}(m_{\tilde{f}_i}^2)) \tag{25}$$

where $\sum_{\tilde{f}_i\tilde{f}_j}(p^2)$, $i,j=1,2$ is the scalar-fermion bare self-energy.

One has then to choose a renormalization condition which defines the mixing angle θ_f. We select this condition in such a way to kill the transitions $\tilde{f}_i \leftrightarrow \tilde{f}_j$ at the one-loop level. The renormalization of the scalar-fermion mixing angle is then given by [14]

$$\delta\theta_f = \frac{1}{2}\frac{\Sigma_{\tilde{f}_i\tilde{f}_j}(m^2_{\tilde{f}_j}) + \Sigma_{\tilde{f}_i\tilde{f}_j}(m^2_{\tilde{f}_i})}{m^2_{\tilde{f}_j} - m^2_{\tilde{f}_i}}. \tag{26}$$

IV. NUMERICS

Now we are ready to present our numerical results both for the tree-level and one-loop decay widths and branching ratios for $\tilde{f}_i \to \tilde{f}_j Z$ and $\tilde{f}_i \to \tilde{f}'_j W^{\pm}$. Let us first fix our inputs and SUSY parameters choice.

As experimental data points [31], the following input quantities enter: $\alpha^{-1} = 137.03598$, $m_Z = 91.1875$ GeV, $m_W = 80.45$ GeV. Fermion masses are given by

$$m_e = 0.000511 \text{ GeV}, \qquad m_\mu = 0.1056 \text{ GeV},$$
$$m_\tau = 1.777 \text{ GeV}, \qquad m_t = 178 \text{ GeV},$$
$$m_b = 4.7 \text{ GeV}, \qquad m_c = 1.5 \text{ GeV},$$
$$m_u = 0.062 \text{ GeV}, \qquad m_d = 0.083 \text{ GeV},$$
$$m_s = 0.215 \text{ GeV}$$

where effective quark masses reproducing the hadronic vacuum polarization contribution $\Delta\alpha(m_Z^2)$ with a sufficiently high accuracy have been chosen [32].

For the SUSY parameters, we will use MSSM inputs which look like some of the Snow-mass Points and Slopes (SPS) and benchmark scenarios for SUSY searches [18]. For our study we will use SPS1 and SPS5 scenarios. As we explained in the introduction, for those 2 scenarios the bosonic decays of scalar fermions $\tilde{f}_i \to \tilde{f}_j V$, when open, are dominant. More details about the mass spectrum and decay rates can be found in [18,19].

In SPS1, we have the following spectrum (only the parameters needed are listed): $\tan\beta = 10$, $m_{A^0} = 394$ GeV, $A_t = -431.34$ GeV, $A_b = 582.67$ GeV, $M = 193$ GeV, $M' = 99$ GeV, $\mu = 352$ GeV. The mass of the first and second generation scalar fermion is of the order 177 GeV (average), while the masses of the third-generation scalar fermions are $m_{\tilde{t}_1} = 396.43$ GeV, $m_{\tilde{t}_2} = 574.71$ GeV, $m_{\tilde{b}_1} = 491.91$ GeV, $m_{\tilde{b}_2} = 524.59$ GeV. The mixing angles are given by $\cos\theta_t = 0.57$, $\cos\theta_b = 0.88$.

In SPS5 (light stop scenario), we have the following spectrum: $m_{A^0} = 694$ GeV, $\tan\beta = 5$ $A_t = -785.57$ GeV, $A_b = -139.11$ GeV, $M = 235$ GeV, $M' = 121$ GeV, $\mu = 640$ GeV. The mass of the first and second generation scalar fermion is of the order 231 GeV (average). The masses of the third generation are $m_{\tilde{t}_1} = 253.66$ GeV, $m_{\tilde{t}_2} = 644.65$ GeV, $m_{\tilde{b}_1} = 535.86$ GeV, $m_{\tilde{b}_2} = 622.99$ GeV. The mixing angles are given by $\cos\theta_t = 0.54$, $\cos\theta_b = 0.98$.

In fact, our strategy is the following: the SPS1 and SPS5 outputs are fixed as above, but we will allow a variation of the mixing angles $\cos\theta_t$, $\cos\theta_b$ from their SPS values. According to our parametrization defined in Sec. II, we choose as independent parameters $m_{\tilde{t}_2}, m_{\tilde{b}_1} m_{\tilde{b}_2}, \theta_t, \theta_b$ together with μ and $\tan\beta$. $m_{\tilde{t}_1}$ is fixed by Eq. (8) and the soft trilinear parameters are fixed using Eq. (9). The variation of $\cos\theta_t$ and $\cos\theta_b$ imply the variation of $m_{\tilde{t}_2}$ as well as A_t and A_b. Since we allow variation of the $\cos\theta_t$ and $m_{\tilde{t}_2}$ mass, our inputs can be viewed as a general MSSM input and not as a SPS one.

As outlined in Sec. II, $A_{t,b}$ are fixed by tree-level relation equation (9). Of course, $A_{t,b}$ receive radiative corrections at high order. However, A_t and A_b enter the game only at one-loop level in our processes; radiative corrections to A_t and A_b are considered as two-loop effects. Before presenting our results, we would like to mention that we neglect radiative corrections to Eq. (8). As mentioned in Sec. II, the one-loop effect to Eq. (8) can shift the tree-level masses only by less than $\lesssim 10$ GeV. We have checked that for our process such shift does not significantly affect our result.

In Fig. 4 we show branching ratios of $\tilde{b}_1$, $\tilde{b}_2$, and $\tilde{t}_2$. We evaluate the bosonic decays $\tilde{b}_1 \to W^-\tilde{t}_1$, $\tilde{b}_2 \to W^-\tilde{t}_1$, and $\tilde{t}_2 \to Z^0\tilde{t}_1$ as well as the fermionic decays $\tilde{f}_i \to \chi_i^0 f(\chi_i^+ f')$ as a function of $\cos\theta_t$ for SPS1 (left) and SPS5 (right) scenarios. From those plots, it is clear that the bosonic decays, once open, are the dominant ones for $|\cos\theta_t| \approx 0.4$–$0.45$. For $|\cos\theta_t| \approx 0.4$ the light stop $m_{\tilde{t}_1}$ is about 100 GeV; when $|\cos\theta_t|$ increases, the $m_{\tilde{t}_1}$ increases also and for large $|\cos\theta_t|$ the bosonic decays are already close and the branching ratio vanishes.

We note that in the case of SPS1 the bosonic decays are open only for $0.4 \lesssim |\cos\theta_t| \lesssim 0.6$, Fig. 4 (left). In the region $|\cos\theta_t| \lesssim 0.4$, the light stop is below the experimental upper limit $m_{\tilde{t}_1} \approx 90$ GeV, and no data are shown. While in the case of SPS5, Fig. 4 (right), for $|\cos\theta_t| \lesssim 0.5$, we find that $m_{\tilde{t}_1}$ is below the experimental upper limit and also $\delta\rho \gtrsim 0.001$ due to large splitting between stops and sbottoms.

The magnitude of SUSY radiative corrections can be described by the relative correction which we define as

$$\Delta = \frac{\Gamma^{1-\text{loop}}(\tilde{f}_i \to \tilde{f}_j V) - \Gamma^{\text{tree}}(\tilde{f}_i \to \tilde{f}_j V)}{\Gamma^{\text{tree}}(\tilde{f}_i \to \tilde{f}_j V)}. \tag{27}$$

In Fig. 5 we illustrate the relative correction Δ as a function of $\cos\theta_t$ for the decay $\tilde{b}_2 \to W\tilde{t}_1$ in SPS1 (left) and SPS5 (right). As it can be seen from the left plot, the SUSY-QCD corrections lie in the range -1%– -6% while

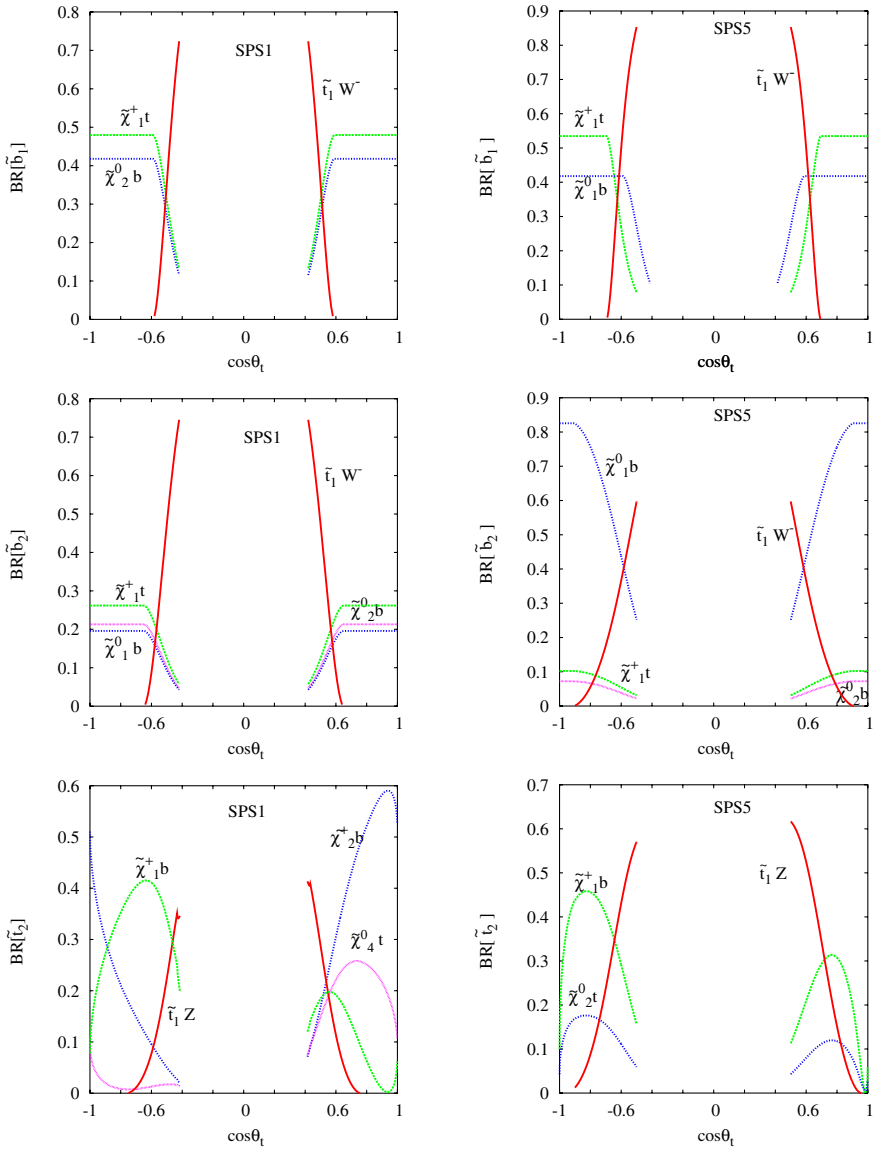

FIG. 4 (color online). Branching ratios of bosonic decays of $\tilde{b}_1$ (upper plots), $\tilde{b}_2$ (middle plots), and $\tilde{t}_2$ (lower plots) in SPS1 (left) and SPS5 (right) as a function of $\cos\theta_t$.

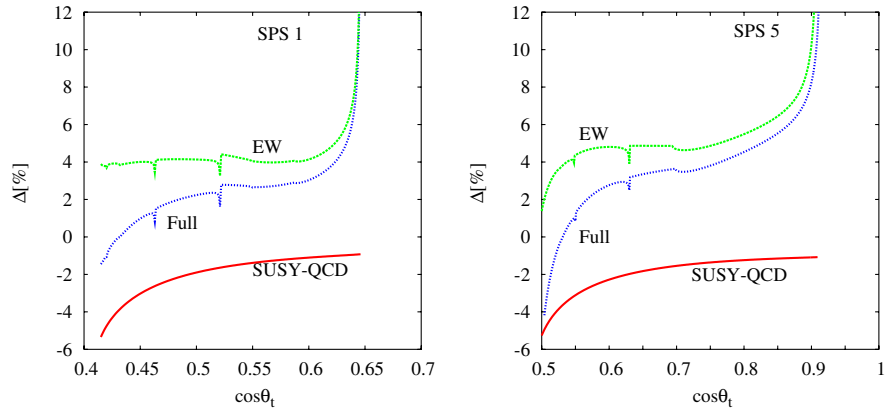

FIG. 5 (color online). Relative correction (EW, SUSY-QCD, and full) to $\tilde{b}_2 \to \tilde{t}_1 W$ as a function of $\cos\theta_t$ in SPS1 (left) and SPS5 (right).

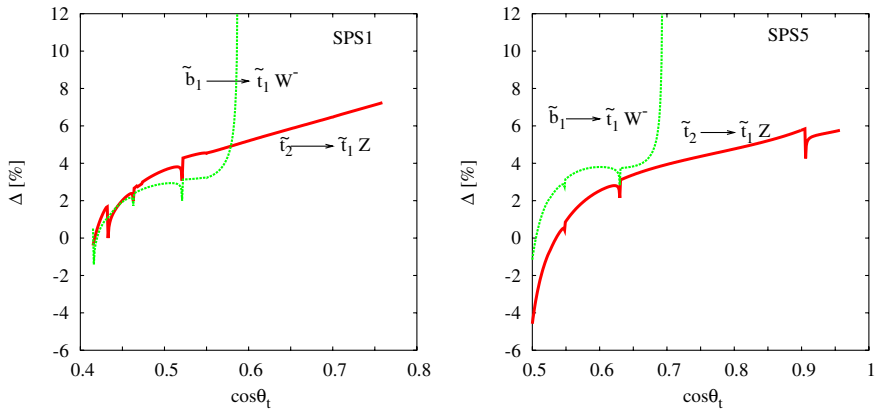

FIG. 6 (color online). Relative correction to $\tilde{b}_1 \to \tilde{t}_1 W$ and $\tilde{t}_2 \to \tilde{t}_1 Z$ as a function of $\cos\theta_t$ in SPS1 (left) and SPS5 (right).

the EW corrections lie in the range 4%–10% for $\cos\theta_t \approx 0.4$–0.65. The SUSY-QCD and EW corrections are of opposite sign; there is a destructive interference and so the full one-loop corrections lie between them. For $\cos\theta_t \to 0.65$, the total correction increases to about 10%. This is due to the fact that for $\cos\theta_t \to 0.65$ the mass of light stop is $m_{\tilde{t}_1} \approx 444$ GeV; the decay $\tilde{b}_2 \to W\tilde{t}_1$ is closed and so the tree-level width decreases to zero. The observed peaks around $\cos\theta_t \approx 0.46$ (resp. $\cos\theta_t \approx 0.53$) correspond to the opening of the transition $\tilde{t}_1 \to \chi_1^0 t$ (resp. $\tilde{t}_1 \to \chi_2^0 t$). The right plot of Fig. 5 in the SPS5 scenario exhibits almost the same behavior as the left plot. The electroweak corrections interfere destructively with the SUSY-QCD ones; the full corrections are between -4%–10% for $\cos\theta_t \in [0.5, 0.9]$.

In Fig. 6 we show the relative correction Δ as a function of $\cos\theta_t$ for the decay $\tilde{b}_1 \to W\tilde{t}_1$ and $\tilde{t}_2 \to Z\tilde{t}_1$ in SPS1 (left) and SPS5 (right) scenarios.

In the case of $\tilde{t}_2 \to Z\tilde{t}_1$, the total correction lies in -1%–7% (resp. -5–6%) in the SPS1 (resp. SPS5) scenario. From Fig. 6, one can see that the relative corrections for $\tilde{b}_1 \to W\tilde{t}_1$ are enhanced for $\cos\theta_t \approx 0.6$ (resp. $\cos\theta_t \approx 0.75$) in SPS1 (resp. SPS5). This behavior has the same explanation as for $\tilde{b}_2 \to W\tilde{t}_1$ in Fig. 5. At $\cos\theta_t \approx 0.6$ (resp. $\cos\theta_t \approx 0.75$) in SPS1 (resp. SPS5), the decay channel $\tilde{b}_1 \to W\tilde{t}_1$ (resp. $\tilde{t}_2 \to Z\tilde{t}_1$) is closed and so the tree-level width decreases to zero. The observed peaks around $\cos\theta_t \approx 0.46$ (resp. $\cos\theta_t \approx 0.53$) correspond to the opening of the transition $\tilde{t}_1 \to \chi_1^0 t$ (resp. $\tilde{t}_1 \to \chi_2^0 t$).

In all cases, we have isolated the QED corrections (virtual photons and real photons); we have checked that this contribution is very small, less than about 1%.

Figure 7 illustrates the relative corrections to $\tilde{t}_2 \to \tilde{b}_1 W$, $\tilde{t}_2 \to \tilde{t}_1 Z$ (left) and $\tilde{b}_2 \to \tilde{b}_1 Z$, $\tilde{b}_2 \to \tilde{t}_1 W$ (right) as a function of $A_b = A_t$ in general MSSM for large $\tan\beta = 60$, $\mu = 500$ GeV, $M_2 = 130$ GeV, and $M_A = 200$ GeV. It is clear from this plot that the relative corrections are bigger than in the cases of SPS scenarios. This enhancement shows up for large $|A_b|$ and also near threshold regions. In this scenario, the SUSY-QCD corrections are about 2%, the electroweak corrections are about 5%, while the QED

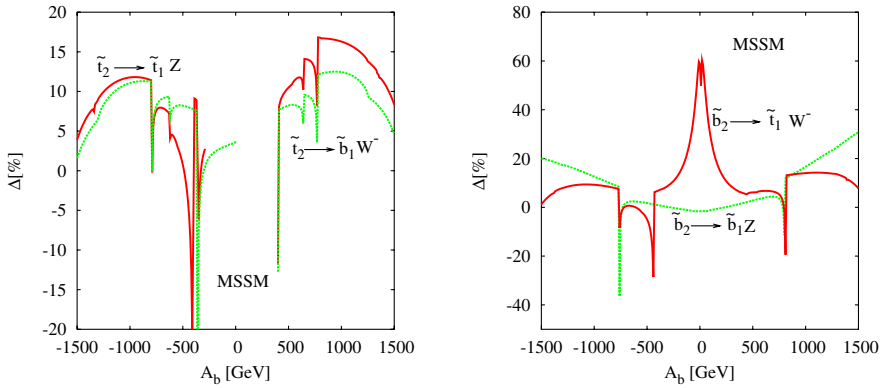

FIG. 7 (color online). Relative correction to $\tilde{t}_2 \to \tilde{b}_1 W$, $\tilde{t}_2 \to \tilde{t}_1 Z$ (left) and $\tilde{b}_2 \to \tilde{b}_1 Z$, $\tilde{b}_2 \to \tilde{t}_1 W$ (right) as a function of $A_t = A_b$ in general MSSM for $\mu = 500$ GeV, $M_2 = 130$ GeV, $M_A = 200$ GeV, and $\tan\beta = 60$.

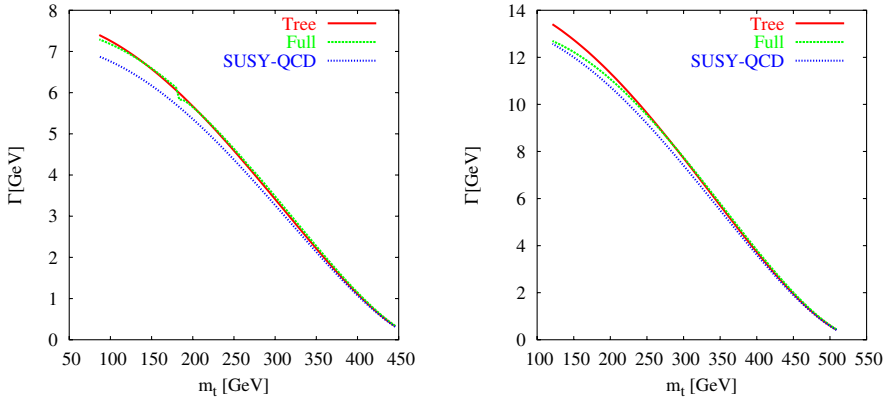

FIG. 8 (color online). Tree and one-loop decay width of $\tilde{t}_2 \to \tilde{t}_1 Z$ as a function of $m_{\tilde{t}_1}$.

corrections are very small. The dominant contribution comes from the Yukawa corrections and is enhanced by large $\tan\beta = 60$ and large $|A_b|$.

In the left plot of Fig. 7, the region $|A_b| = |A_t| <$ 300 GeV has no data. This is due to the fact that splitting between $\tilde{t}_2$ and $\tilde{t}_1$ ($\tilde{t}_2$ and $\tilde{b}_1$) is not large enough to allow the decays $\tilde{t}_2 \to \tilde{t}_1 Z$ and $\tilde{t}_2 \to \tilde{b}_1 W$.

In the right plot of Fig. 7, when $|A_b| = |A_t| \approx 0$ GeV, the splitting between $\tilde{b}_2$ and $\tilde{t}_1$ is close to m_W mass and so the tree-level width for $\tilde{b}_2 \to \tilde{t}_1 W^+$ almost vanishes; consequently the correction is getting bigger. This behavior has also been observed in previous plots for $\tilde{b}_2 \to \tilde{t}_1 W^+$.

Finally, in Fig. 8 we illustrate the decay width of $\tilde{t}_2 \to \tilde{t}_1 Z$ as a function of $m_{\tilde{t}_1}$ in SPS1 (left) and SPS5 (right). In SPS1 (resp. SPS5) the decay width of $\tilde{t}_2 \to \tilde{t}_1 Z$ is about 8 GeV (resp. 13 GeV) for light stop mass of the order 100 GeV. Obviously, these decay widths decrease as the light stop mass increases.

It is clear that the SUSY-QCD corrections reduce the width while the electroweak corrections cancel part of those QCD corrections. Both in SPS1 and SPS5, the full one-loop width of $\tilde{t}_2 \to \tilde{t}_1 Z$ is in some cases slightly bigger than the tree-level width.

V. CONCLUSIONS

Full one-loop calculations of third-generation scalar-fermion decays into gauge bosons W and Z are presented in the on-shell scheme. We include electroweak, QED, and SUSY-QCD contributions to the decay width. It is found that the QED corrections are rather small while the electroweak and SUSY-QCD corrections interfere destructively.

The size of the one-loop effects are typically of the order -5%–10% in SPS scenarios which are based on SUGRA assumptions. In model independent analysis like the general MSSM, the size of the corrections are bigger and can reach about 20% for large $\tan\beta$ and large soft SUSY-breaking A_b. Their inclusion in phenomenological studies and analyses are then well motivated.

ACKNOWLEDGMENTS

The authors thank ICTP for the warm hospitality extended to them during the first stage of this work. We thank Margarete Muhlleitner for useful exchange of informations about Sdecay [23]. This work is supported by PROTARS-III D16/04.

[1] H. E. Haber and G. L. Kane, Phys. Rep. **117**, 75 (1985); H. P. Nilles, Phys. Rep. **110**, 1 (1984); P. Nath, R. Arnowitt, and A. Chamseddine, *Applied $N = 1$ Supergravity*, ITCP Series in Theoretical Physics (World Scientific, Singapore, 1984); X. R. Tata, in *Proceedings of the Mt. Sorak Symposium on the Standard Model and Beyond, Mt Sorak, Korea, 1990.*

[2] CDF Collaboration, T. Affolder *et al.*, Phys. Rev. D **63**, 091101 (2001); hep-ex/0011004; OPAL Collaboration, G. Abbiendi *et al.*, Phys. Lett. B **545**, 272 (2002); **548**, 258(E) (2002).

[3] F. del Aguila and L. Ametller, Phys. Lett. B **261**, 326 (1991); H. Baer, C. h. Chen, F. Paige, and X. Tata, Phys. Rev. D **49**, 3283 (1994).

[4] ECFA/DESY LC Physics Working Group Collaboration, J. A. Aguilar-Saavedra *et al.*, hep-ph/0106315; ACFA Linear Collider Working Group Collaboration, K. Abe *et al.*, hep-ph/0109166; American Linear Collider Working Group CollaborationT. Abe *et al.*, in *Proceedings of the APS/DPF/DPB Summer Study on the Future of Particle Physics, Snowmass, 2001*, edited by N. Graf, hep-ex/0106056.

[5] W. Beenakker, R. Hopker, M. Spira, and P. M. Zerwas, Nucl. Phys. **B492**, 51 (1997); W. Beenakker, R. Hopker, M. Spira, and P. M. Zerwas, Phys. Rev. Lett. **74**, 2905 (1995).

[6] J. L. Feng and D. E. Finnell, Phys. Rev. D **49**, 2369 (1994); T. Tsukamoto, K. Fujii, H. Murayama, M. Yamaguchi, and Y. Okada, Phys. Rev. D **51**, 3153 (1995); R. Keranen, A. Sopczak, H. Nowak, and M. Berggren, Eur. Phys. J. direct C **2**, 7 (2000); R. Kitano, T. Moroi, and S. f. Su, J. High Energy Phys. 12 (2002) 011; E. L. Berger, J. Lee, and T. M. Tait, Phys. Rev. D **69**, 055003 (2004).

[7] A. Arhrib, M. Capdequi-Peyranere, and A. Djouadi, Phys. Rev. D **52**, 1404 (1995); M. Drees and K. I. Hikasa, Phys. Lett. B **252**, 127 (1990).

[8] H. Eberl, A. Bartl, and W. Majerotto, Nucl. Phys. **B472**, 481 (1996).

[9] A. Freitas *et al.*, hep-ph/0211108; A. Freitas, D. J. Miller, and P. M. Zerwas, Eur. Phys. J. C **21**, 361 (2001).

[10] A. Arhrib and W. Hollik, J. High Energy Phys. 04 (2004) 073.

[11] H. Eberl, S. Kraml, and W. Majerotto, J. High Energy Phys. 05 (1999) 016; K. Kovarik, C. Weber, H. Eberl, and W. Majerotto, Phys. Lett. B **591** , 242 (2004).

[12] M. Beccaria, M. Melles, F. M. Renard, S. Trimarchi, and C. Verzegnassi, Int. J. Mod. Phys. A **18**, 5069 (2003).

[13] A. Djouadi, W. Hollik, and C. Junger, Phys. Rev. D **55**, 6975 (1997); S. Kraml, H. Eberl, A. Bartl, W. Majerotto, and W. Porod, Phys. Lett. B **386**, 175 (1996).

[14] J. Guasch, W. Hollik, and J. Sola, J. High Energy Phys. 10 (2002) 040; Phys. Lett. B **437**, 88 (1998).

[15] A. Arhrib, A. Djouadi, W. Hollik, and C. Junger, Phys. Rev. D **57**, 5860 (1998).

[16] A. Bartl, H. Eberl, S. Kraml, W. Majerotto, W. Porod, and A. Sopczak, Z. Phys. C **76**, 549 (1997).

[17] A. Bartl, H. Eberl, K. Hidaka, S. Kraml, W. Majerotto, W. Porod, and Y. Yamada, Phys. Lett. B **419**, 243 (1998).

[18] B. C. Allanach *et al.*, Eur. Phys. J. C **25**, 113 (2002).

[19] N. Ghodbane and H. U. Martyn, in *Proceedings of the APS/DPF/DPB Summer Study on the Future of Particle Physics, Snowmass, 2001*, edited by N. Graf, hep-ph/0201233.

[20] W. Hollik and H. Rzehak, Eur. Phys. J. C **32**, 127 (2003).

[21] C. Kounnas, A. B. Lahanas, D. V. Nanopoulos, and M. Quiros, Nucl. Phys. **B236**, 438 (1984); J. F. Gunion, H. E. Haber, and M. Sher, Nucl. Phys. **B306**, 1 (1988); J. A. Casas, A. Lleyda, and C. Munoz, Nucl. Phys. **B471**, 3 (1996).

[22] A. Djouadi, J. L. Kneur, and G. Moultaka, hep-ph/0211331.

[23] M. Muhlleitner, A. Djouadi, and Y. Mambrini, hep-ph/0311167.

[24] J. Kublbeck, M. Bohm, and A. Denner, Comput. Phys. Commun. **60**, 165 (1990); T. Hahn, Comput. Phys. Commun. **140**, 418 (2001); T. Hahn and C. Schappacher, Comput. Phys. Commun. **143**, 54 (2002); T. Hahn and M. Perez-Victoria, Comput. Phys. Commun. **118**, 153 (1999).

[25] G. J. van Oldenborgh, Comput. Phys. Commun. **66**, 1 (1991); T. Hahn, Acta Phys. Pol. B **30**, 3469 (1999).

[26] W. Siegel, Phys. Lett. B **84**, 193 (1979); D. M. Capper, D. R. Jones, and P. van Nieuwenhuizen, Nucl. Phys. **B167**, 479 (1980).

[27] A. Denner, Fortschr. Phys. **41**, 307 (1993).

[28] W. Hollik, E. Kraus, M. Roth, C. Rupp, K. Sibold, and D. Stockinger, Nucl. Phys. **B639**, 3 (2002).

[29] W. Majerotto, hep-ph/0209137.

[30] T. Fritzsche and W. Hollik, Eur. Phys. J. C **24**, 619 (2002).

[31] Particle Data Group Collaboration, K. Hagiwara *et al.*, Phys. Rev. D **66**, 010001 (2002).

[32] S. Eidelman and F. Jegerlehner, Z. Phys. C **67**, 585 (1995); D. Bardin *et al.*, CERN Report No. 95-03, 1995, edited by D. Bardin, W. Hollik, and G. Passarino, pp. 7–162, hep-ph/9709229.